Supporting Information

Chen et al. 10.1073/pnas.1715625115

SI Methods

Subjects and Preparation. Extracellular recordings were made from two male rhesus monkeys (*Macaca mulatta*), weighing 7–10 kg. The monkeys were chronically implanted with a circular delrin ring for head stabilization, as well as two scleral search coils for measuring binocular eye position. Details have been described (1–5).

Apparatus and Vestibular Stimulus. Each animal was seated comfortably in a primate chair, and their head was fixed to the chair via a light-weight plastic ring that was anchored to the skull using titanium inverted T-bolts and dental acrylic. The primate chair was secured on top of a computer-controlled yaw motor that could be used to passively rotate the animal's head and body inside a cubic magnetic field coil frame (CNC Engineering; used to measure eye movements). Attached to the front surface of the coil frame was a rear-projection screen that was positioned 30 cm in front of the monkey and subtended 90° × 90° of visual angle. The other sides of the coil frame were covered with black, nonreflective material, such that the monkey's field of view was restricted to the visual display and the local environment within the coil frame. The coil frame, display screen, and a stereoscopic video projector (described below) were firmly mounted on top of a six-degree-of-freedom motion platform (MOOG 6DOF2000E; Moog) that allowed physical translation of the animal (3, 4). Together, the motion platform and coil frame defined a visual allocentric reference frame. Rotations of the yaw motor changed the orientation (angular position) of the body relative to this allocentric reference frame, and movements of the motion platform translated the entire allocentric frame relative to the world.

A video projector (Christie Digital Mirage 2000; Christie) was mounted on the motion platform and was used to rear-project a fixation target onto the screen. No visual stimuli were presented on the screen other than the fixation target, but the background illumination from the projector allowed animals to register multiple allocentric cues within the local environment on top of the motion platform. As a result, when the yaw rotator was used to change the orientation of the animal's head and body relative to the motion platform (see below), visual cues were informative regarding body orientation relative to the allocentric frame defined by the coil frame and motion platform.

Experimental Protocol. Translation of the animal by the motion platform followed a Gaussian velocity profile with a duration of 1 s, a displacement of 13 cm, a peak acceleration of ≅0.1G (0.98 m/s^2), and a peak velocity of 0.30 m/s (4). Translation was limited to the horizontal plane in this study, and 10 different azimuth angles (relative to the world) were tested (0°, 45°, 70°, 90°, 110°, 135°, 180°, 225°, 270°, and 315°), where 0° corresponds to rightward and 90° corresponds to forward. The directions 20° to the left and right of straight ahead (70° and 110°) were included to align with the directions of the eccentric eye targets.

At the start of each trial, the monkey's body (together with the monkey chair) was rotated by using the yaw motor to one of three orientations (relative to the world): −20° (left), 0° (straight ahead), or +20° (right). Then, 1,000 ms after the end of yaw rotation, a fixation target appeared on the screen (orange square; Fig. 1). The monkey was required to fixate the target, within a 2° × 2° window, for 300 ms before stimulus onset and to maintain fixation throughout the 1-s translational motion stimulus, as well as for an additional 0.5 s after translation ended. A juice reward was given after each successful trial. At the end of each trial, the monkey chair was rotated back to its original position (0°). Note that an eye calibration process was performed for each of the three body-in-world orientations (left, straight ahead, and right), and the corresponding calibration parameters were used to calculate eye position accurately for each body orientation.

To distinguish body- and world-centered reference frames, body orientation relative to the world was varied randomly across trials (−20°, 0°, or 20°) by rotating the monkey chair, while keeping head position relative to the body fixed. However, by manipulating the fixation target on the screen, we could compare a body-fixed gaze condition (including three [body-in-world, eye-in-head] positions: [−20°, 0°], [0°, 0°], [20°, 0°]) and a world-fixed gaze condition (including three [body-in-world, eye-in-head] positions: [−20°, 20°], [0°, 0°], [20°, −20°]). Since [0°, 0°] appears in both conditions, there were a total of five distinct combinations of [body-in-world, eye-in-head] positions: [−20°, 0°], [−20°, 20°], [0°, 0°], [20°, −20°], [20°, 0°], which were randomly interleaved in a single block of trials.

Neural Recordings. A plastic grid made from Delrin (3.5 × 5.5 × 0.5 cm), containing staggered rows of holes (0.8-mm spacing), was stereotaxically attached to the inside of the head-restraint ring by using dental acrylic and was positioned to overlay VIP in both hemispheres. Area VIP was initially localized via structural MRI scans (3, 6), and this localization was refined by the patterns of white and gray matter transition, as well as neuronal response properties, as described (1, 4, 5).

Recordings were made by using tungsten microelectrodes (FHC) that were inserted into the brain via transdural guide tubes. Each neuron was first tested, in complete darkness (projector off), with sinusoidal vestibular stimuli involving translation (0.5 Hz, ±10 cm) along the lateral and forward/backward directions. Only neurons with clear response modulations to sinusoidal vestibular stimuli were further tested with the heading tuning protocol described above. Data were collected from four hemispheres of two monkeys, F ($n = 55$) and X ($n = 54$). Results were similar in the two monkeys; thus, data were pooled across monkeys for all population analyses.

Data Analysis. All data analyses were done in Matlab (MathWorks). Neurons included in population analyses were tested with at least three repetitions of each of the 50 distinct stimulus combinations (10 heading directions × 5 body/eye position combinations) ($n = 50$ from monkey F, 52 from monkey X) and five or more repetitions were obtained for most neurons (84.3%). For each stimulus combination (Fig. 2*A*), peristimulus time histograms were constructed by grouping spikes into 50-ms time bins and then smoothed by a 100-ms boxcar filter. For each body/eye position combination (Fig. 2 *B* and *C*), a heading tuning curve was constructed by plotting firing rate as a function of heading. Firing rates were computed in a 400-ms window centered on the "peak time" (7). To identify peak time, firing rates were computed in many different 400-ms time windows spanning the range of the data in 25-ms steps. The peak time was defined as the center of the 400-ms window for which the neural response reached its maximum across all body/eye position combinations. For each 400-ms window, a one-way ANOVA (response by heading direction) was performed for each body/eye position combination. Heading tuning was considered statistically significant if the one-way ANOVA passed the significance test ($P < 0.05$) for five contiguous time points centered on the peak time. Only neurons with significant tuning for at least

two of the three body/eye position combinations in either the body- or world-fixed gaze condition were included in the reference frame analyses described below.

DI computation. The shift of heading tuning curves relative to the change in body orientation was assessed by using a DI, which was computed by the following equation (2, 8):

$$(DI)_{ij} = \frac{k^{\max\left(cov\left[R_i(\theta), R_j(\theta+k)\right]\right)}}{P_i - P_j}. \quad \textbf{[S1]}$$

Tuning data were linearly interpolated to 1° resolution before the computation of DI, and results were quite robust to the choice of interpolation resolution as long as the data were interpolated to a resolution of ~10° or less (Fig. S5). Here, k (in degrees) is the shift between a pair of tuning curves (denoted R_i and R_j), and the superscript above k refers to the maximum covariance between the tuning curves as a function of k (ranging from −180° to +180°). The denominator represents the difference between the body orientations (P_i and P_j) at which the tuning functions were measured. DI ranges between 1 (when the tuning curve shifts by an amount equal to the change in body orientation) and 0 (when there is no shift with body orientation). In practice, however, DI values could be <0 or >1 because of variability in neural responses. A single average DI was computed for each condition (body- and world-fixed gaze) if all three pairs of tuning curves passed the significance criterion (such that the resulting three DI values were averaged). If only one tuning curve passed the significance criterion (as defined above), this neuron/condition was not included in the DI analysis. The numbers of neurons that met these criteria and were included in the analysis were as follows: body-fixed gaze condition: n = 60 (20 from monkey F, 40 from monkey X); world-fixed gaze condition: n = 61 (21 from monkey F, 40 from monkey X).

A CI was computed for the DI in each condition using a bootstrap method. Bootstrapped tuning curves were generated by resampling (with replacement) the data for each heading and then a DI value was computed for each bootstrapped tuning curve. This was repeated 1,000 times to produce a distribution of bootstrap DI values from which a 95% CI was derived (percentile method). A DI value was considered significantly different from a particular value (0 and/or 1) if its 95% CI did not include that value. A neuron was classified as body-centered in the body- or world-fixed gaze condition if the CI did not include 0 but included 1. A neuron was classified as world-centered in either condition if the CI did not include 1 but included 0. Finally, neurons were classified as having intermediate reference frames if the CI was contained within the interval between 0 and 1, without including 0 or 1. All other cases were designated as unclassified (e.g., neurons for which the CI on DI included both 0 and 1).

Potential asymmetries in tuning shifts were evaluated by comparing the DI value computed from the pairing of left and center body orientations (DI_l) with the DI value computed from the pairing of right and center body orientations (DI_r). For each neuron, DI_l and DI_r were computed for each of 1,000 bootstrapped tuning curves to generate two DI distributions. The tuning shifts were considered asymmetric if 95% CIs for the distributions of DI_l and DI_r did not overlap. To be included in this analysis, all three tuning curves in each condition needed to meet the significance test described above. This resulted in a sample size of n = 57 (20 from monkey F and 37 from monkey X) for the body-fixed gaze condition, and a sample size of n = 52 (18 from monkey F and 34 from monkey X) for the world-fixed gaze condition.

Note that changes in eye position were not considered in the DI computation for the world-fixed gaze condition, although eye-in-head and body-in-world positions covaried in that condition. In our previous study (4), vestibular heading signals were found to be independent of gaze direction; thus, we expected that tuning curves would not change with eye-in-head position. As a result, the DI was computed only relative to the change in body-in-world position in the world-fixed gaze condition.

Fitting tuning curves independently. Each tuning curve was fit independently with a von Mises function (2):

$$R(\theta) = A \cdot e^{\frac{-(1-\cos(\theta-\theta_p))}{2\sigma^2}} + r_b, \quad \textbf{[S2]}$$

where A is the response amplitude, θ_p is the preferred heading, σ is the tuning width, and r_b is the baseline response level. von Mises functions provide excellent fits to the heading data when all parameters are free (median values of R^2: 0.94, 0.94, 0.95, 0.95, and 0.95 for each of the five combinations of body/eye positions).

Values of A were used to quantify gain field effects. Specifically, in each task condition (body- and world-fixed gaze) for each neuron, gain ratios between left (−20°) and center (0°) body positions (A_{L20}/A_0) and between right (20°) and center body positions (A_{R20}/A_0) were computed. A bootstrap method was used to evaluate the significance of gain field effects. Specifically, bootstrapped tuning curves were generated by resampling (with replacement) the data for each heading, and then each bootstrapped tuning curve was fit independently with Eq. **S2**, and the gain ratios were computed. This was repeated 1,000 times to generate bootstrap distributions of A_{L20}/A_0 and A_{R20}/A_0. If the 95% CI on the gain ratio did not include 1 for either A_{L20}/A_0 or A_{R20}/A_0, the gain field effect was considered significant. To be included in this analysis, all three tuning curves in each condition also needed to meet the two requirements described above. Only significant gain fields for both conditions were used for comparisons between conditions (n = 50: 17 from monkey F and 33 from monkey X).

Fitting tuning curves with body- and world-centered models. For each neuron, to determine to what extent the whole set of tuning curves in each condition (body- and world-fixed gaze) was more consistent with a body- or world-centered representation, the three tuning curves in each condition were also fitted simultaneously with a set of von Mises functions (2). Tuning curves from the body- and world-fixed gaze conditions were fit with a body-centered model and a world-centered model, in which A, σ, and r_b were free parameters for each body/eye position, and only θ_p was controlled. Specifically, θ_p was constrained to shift by exactly the amount of the body orientation change (i.e., θ_p for straight forward, θ_p + 20° for leftward, and θ_p − 20° for rightward) in the body-centered model, but was constrained to be constant (θ_p) for all three tuning curves (no shift) in the world-centered model. Thus, the total number of free parameters for each model was 10 (three free parameters × three tuning curves +θ_p).

Neurons included in this model-fitting analysis needed to meet two requirements: (*i*) All three tuning curves passed the significance criteria described above, and (*ii*) all three tuning curves were well-fit separately (i.e., when all four parameters were free) by the function of Eq. **S2**, as indicated by individual R^2 values >0.6. The numbers of neurons that passed both criteria were as follows: body-fixed gaze condition: n = 57 (20 from monkey F and 37 from monkey X); world-fixed gaze condition: n = 52 (18 from monkey F and 34 from monkey X).

For each fit, the correlation between the best-fitting function and the data were computed to measure the goodness-of-fit. To remove the influence of correlations between the models themselves, partial correlation coefficients were computed by the Matlab function "partialcorr" and subsequently normalized by using Fisher's r-to-Z transform (2, 9, 10), such that Z scores from the two models could be compared (Fig. 5). If the Z score for one model was >2.326 and exceeded the Z score for the other model by at least 2.326 (equivalent to a P value of 0.01), that

model was considered a significantly better fit to the data than the alternative model (2).

Average heading tuning curves. As another way to assess the shift of vestibular heading tuning at the population level, tuning curves for each body/eye position combination were normalized and averaged. Specifically, for each neuron, the tuning curve measured at body/eye position = [0°, 0°] was shifted to make 0° the preferred heading, and the other two curves were shifted by the same amount to keep the relative positions of the curves constant. Subsequently, the tuning curves were averaged across all neurons for each combination of body/eye position, and DI values were computed (as described above) for the average normalized tuning curves in each stimulus condition (body- and world-fixed gaze). This analysis was also performed on previous data that distinguished eye-vs.-head and head-vs.-body reference frames (4). The numbers of neurons included were as follows: body-fixed gaze condition, $n = 57$ (20 from monkey F and 37 from monkey X); world-fixed gaze condition, $n = 51$ (17 from monkey F and 34 from monkey X); eye-vs.-head condition, $n = 70$ (30 from monkey E and 40 from monkey Q); and head-vs.-body condition, $n = 68$ (30 from monkey E and 38 from monkey Q).

1. Chen X, DeAngelis GC, Angelaki DE (2013) Eye-centered representation of optic flow tuning in the ventral intraparietal area. *J Neurosci* 33:18574–18582.
2. Fetsch CR, Wang S, Gu Y, DeAngelis GC, Angelaki DE (2007) Spatial reference frames of visual, vestibular, and multimodal heading signals in the dorsal subdivision of the medial superior temporal area. *J Neurosci* 27:700–712.
3. Gu Y, Watkins PV, Angelaki DE, DeAngelis GC (2006) Visual and nonvisual contributions to three-dimensional heading selectivity in the medial superior temporal area. *J Neurosci* 26:73–85.
4. Chen X, DeAngelis GC, Angelaki DE (2013) Diverse spatial reference frames of vestibular signals in parietal cortex. *Neuron* 80:1310–1321.
5. Chen X, DeAngelis GC, Angelaki DE (2014) Eye-centered visual receptive fields in the ventral intraparietal area. *J Neurophysiol* 112:353–361.
6. Chen A, DeAngelis GC, Angelaki DE (2011) Representation of vestibular and visual cues to self-motion in ventral intraparietal cortex. *J Neurosci* 31:12036–12052.
7. Chen A, DeAngelis GC, Angelaki DE (2010) Macaque parieto-insular vestibular cortex: Responses to self-motion and optic flow. *J Neurosci* 30:3022–3042.
8. Avillac M, Denève S, Olivier E, Pouget A, Duhamel JR (2005) Reference frames for representing visual and tactile locations in parietal cortex. *Nat Neurosci* 8: 941–949.
9. Angelaki DE, Shaikh AG, Green AM, Dickman JD (2004) Neurons compute internal models of the physical laws of motion. *Nature* 430:560–564.
10. Smith MA, Majaj NJ, Movshon JA (2005) Dynamics of motion signaling by neurons in macaque area MT. *Nat Neurosci* 8:220–228.

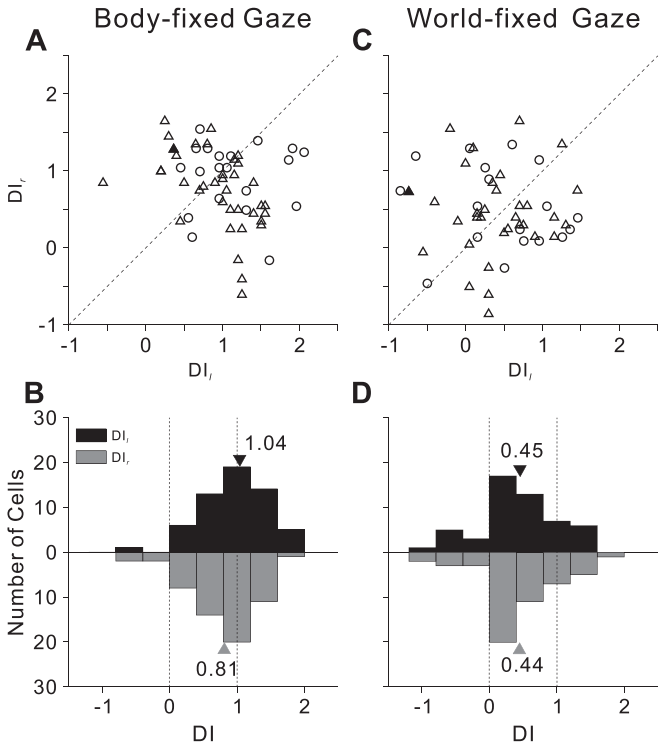

Fig. S1. Analysis of asymmetry in tuning shifts. (*A* and *B*) Body-fixed gaze condition. (*C* and *D*) World-fixed gaze condition. (*A* and *C*) DI values computed from tuning curves for the left and center body orientations (DI_l) are plotted against DI values computed for the right and center orientations (DI_r). Filled symbols indicate DI values that are significantly different for left and right body orientations (body-fixed gaze condition: n = 1/57; world-fixed gaze condition: n = 1/52; bootstrap; *SI Methods*); open symbols indicate DI values that are not significantly different. Circles and triangles denote data from monkeys F and X, respectively. (*B* and *D*) Distributions of DI_l and DI_r for the body-fixed gaze condition (*B*: $n = 57$) and the world-fixed gaze condition (*D*: $n = 52$). The mean of the distributions was slightly different in *B* ($P = 0.04$, *t* test), but not significantly different in *D* ($P = 0.95$). For both conditions, there were no significant differences between the variances of the distributions (*B*: $P = 0.78$; *D*: $P = 0.91$, Levene's test). In the body-fixed gaze condition (*B*), the mean value (arrowhead) was not significantly different from 1 for DI_l (mean = 1.04 ± 0.15, $P = 0.62$, *t* test), but was significantly different from 1 for DI_r (mean = 0.81 ± 0.13, $P = 0.004$). In the world-fixed gaze condition (*D*), both mean values were significantly different from both 0 and 1 (DI_l: mean = 0.45 ± 0.16, $P < 0.001$; DI_r: mean = 0.44 ± 0.17, $P < 0.001$, *t* tests).

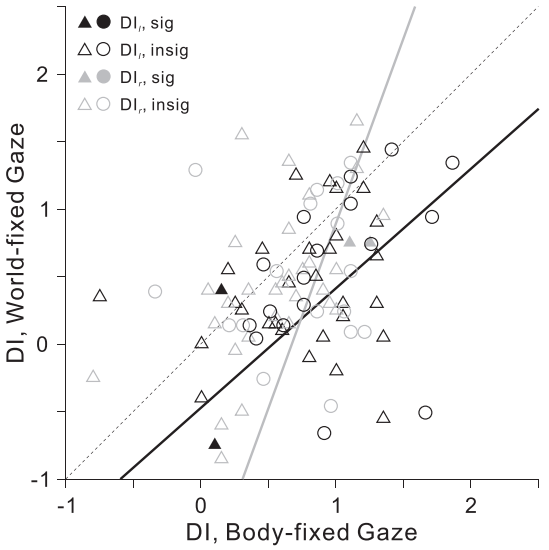

Fig. S2. Comparison of tuning curve shifts across task conditions, separately for left and right body orientations. DI values for the world-fixed gaze condition are plotted against DI values for the body-fixed gaze condition. Black and gray symbols show DI values computed for leftward (DI_l) and rightward (DI_r) body orientations; filled and open symbols indicate data with significant (sig) and insignificant (insig) asymmetric tuning shifts, respectively ($n = 50$). The DI_l and DI_r values in the two task conditions are significantly correlated, and the slopes are not significantly different from unity (type II regression; DI_l : $R = 0.33$, $P = 1.83 \times 10^{-2}$, slope = 0.89, 95% CI = [0.27, 3.05]; DI_r: $R = 0.31$, $P = 2.68 \times 10^{-2}$, slope = 2.73, 95% CI = [1.0, 11.75]). Circles and triangles denote data from monkeys F and X, respectively.

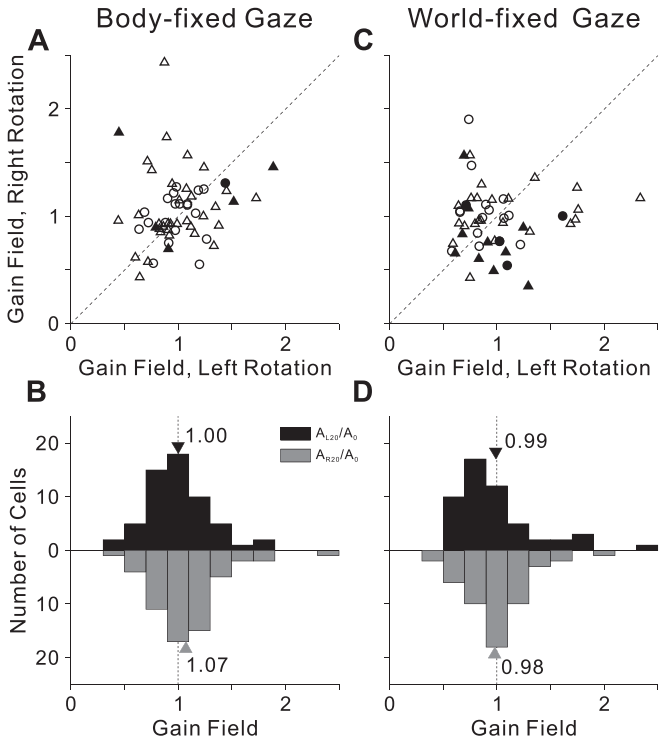

Fig. S3. Summary of gain fields. (*A* and *B*) Body-fixed gaze condition ($n = 57$). (*C* and *D*) World-fixed gaze condition ($n = 52$). (*A* and *C*) The gain ratio for leftward and center body orientations (A_{L20}/A_0) is plotted against the corresponding gain ratio for rightward and center body orientations (A_{R20}/A_0). Filled symbols indicate data with gain ratios that are significantly different from unity for either left or right body orientations; open symbols indicate insignificant gain fields for both body orientations (bootstrap; *SI Methods*). Circles and triangles denote data from monkeys F and X, respectively. Most cells had insignificant gain fields, and only a small percentage of cells had significant gain fields for leftward or rightward body orientations (*A*: 10.5%, 6/57; *C*: 26.9%, 14/52). There was no significant correlation between gain fields for leftward and rightward body orientations (*A*: $R = 0.13$, $P = 0.31$; *C*: $R = 0.01$, $P = 0.93$, type II regression). (*B* and *D*) Distribution of gain fields. For both task conditions, there were no significant differences between the mean values of A_{L20}/A_0 and A_{R20}/A_0 (*B*: $P = 0.20$; *D*: $P = 0.89$, paired *t* tests) or between the variances of the distributions (*B*: $P = 0.48$; *D*: $P = 0.21$, Levene's test). Black and gray bars illustrate gain fields for leftward and rightward body orientations, respectively. The mean values (arrowheads) are not significantly different from 1 (*B*: mean = 1.00 ± 0.08, $P = 0.99$, for left; mean = 1.07 ± 0.09, $P = 0.12$, for right; *D*: mean = 0.99 ± 0.10, $P = 0.86$, for left; mean = 0.98 ± 0.08, $P = 0.65$, for right; *t* test).

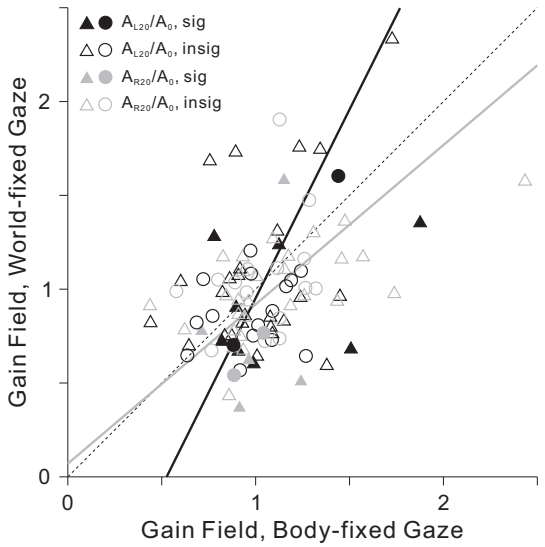

Fig. S4. Comparison of gain fields across task conditions. Gain fields in the world-fixed gaze condition are plotted against gain fields in the body-fixed gaze condition ($n = 50$). Colors show gain fields for leftward (black: A_{L20}/A_0) and rightward (gray: A_{R20}/A_0) body orientations; filled and open symbols indicate data with significant (sig) and insignificant (insig) gain fields, respectively. The gain fields in the two conditions are significantly correlated, and the slopes are not significantly different from unity (type II regression; A_{L20}/A_0: $R = 0.37$, $P = 8.61 \times 10^{-3}$, slope = 2.0, 95% CI = [0.43, 6.83]; A_{R20}/A_0: $R = 0.45$, $P = 1.16 \times 10^{-3}$, slope = 0.85, 95% CI = [0.47, 2.79]). Circles and triangles denote data from monkeys F and X, respectively.

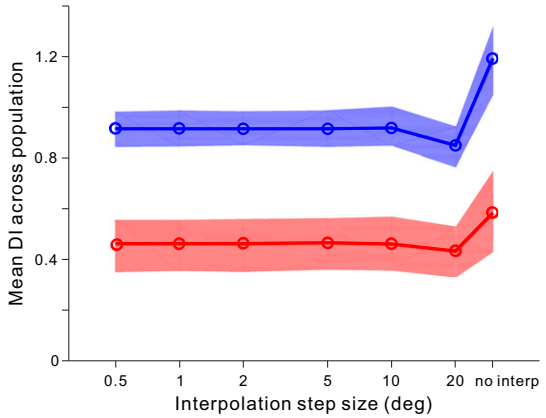

Fig. S5. Distributions of mean DI values across the population for different interpolation step sizes in the DI computation. Colors indicate data for the body-fixed gaze (blue) and world-fixed gaze (red) conditions. Each circle represents the mean DI value across neurons for a particular interpolation step size. "no interp" means that the DI values were computed without any interpolation. Color bands indicate 95% CIs.

Table S1. Comparison of spatial reference frames across the two task conditions of Fig. 3

	World-fixed gaze, *n* (%)				
Body-fixed gaze	Body-centered	Intermediate	Unclassified	World-centered	Total
Body-centered	11 (35.5)	5 (16.1)	10 (32.3)	5 (16.1)	31 (51.7)
Intermediate	0 (0.0)	2 (66.7)	0 (0.0)	1 (33.3)	3 (5.0)
Unclassified	2 (7.7)	0 (0.0)	21 (80.8)	3 (11.5)	26 (43.3)
World-centered	0 (0)	0 (0)	0 (0)	0 (0)	0 (0.0)
Total	13 (21.7)	7 (11.7)	31 (51.7)	9 (15.0)	60

Table S2. Comparison of spatial reference frames across the two task conditions in Fig. 5

	World-fixed gaze, *n* (%)			
Body-fixed gaze	Body-centered	Unclassified	World-centered	Total
Body-centered	7 (20.6)	21 (61.8)	3 (8.8)	34 (58.6)
Unclassified	1 (4.3)	8 (34.8)	9 (39.1)	23 (39.7)
World-centered	1 (100.0)	0 (0.0)	0 (0.0)	1 (1.7)
Total	9 (15.5)	31 (53.4)	12 (20.7)	52